Research on temperature propagation law based on thermite plugging and abandonment technology

Ruitao Sun [1, 2], Jie Zhang [1, 2, *], Zhilin Li [3], Xin Li [1, 2], Huaizhi Tao [3], Sheng Yu [1, 2], Wenzhen Zhang [1, 2]

[1] State Key Laboratory of Oil and Gas Reservoir Geology and Exploitation, South west Petroleum University, Chengdu 610500, Sichuan, P. R. China
[2] Petroleum Engineering School, Southwest Petroleum University, Chengdu 610500, Sichuan, P. R. China
[3] Drilling & Production Engineering Technology Research Institute, Petrochina Chuanqing Drilling Engineering Co., Ltd, Guanghan, 618300, Sichuan, P. R. China

Abstract: The continuous exploration and development of oil wells increases the risk of leakage from abandoned wells and brings challenges to the traditional plugging and abandonment technology. In order to overcome the above problems, a thermite plugging and abandonment technology is proposed in this field. The technology uses the aluminothermic reaction to melt the original or set material for sealing. The natural convection under different confinement conditions directly affects the heat flux transfer in the heat transfer process. In order to study the melting effect of the thermite reaction on sandstone, based on the heat conduction theory, a heat conduction model based on the temperature release law of the thermite reaction was established. The numerical simulation results show that the surrounding heat transfer conditions are the key factors affecting the heat transfer effect in the axial and radial directions without considering the particle size and dosage of the thermite itself. This work is of great significance for studying the temperature law of thermite reaction release and the future research of thermite plugging and abandonment technology.

Keywords: Thermite plugging and abandonment technology; natural convection under; closed environment; Aluminothermic melting effect.

1. Introduction

Permanent P&A operations on abandoned wells are designed to isolate and seal the permeable sections of the underground rock formation. This operation is carried out to prevent underground fluids from flowing upward into the aquifer and being discharged to the surface. However, the P&A operation does not produce any economic benefits. The operation has been carried out at the lowest cost due to the early oil and gas well depth and the ambiguity of the plugging and abandonment standards [1]. The downhole environment has gradually developed into complex conditions, such as deep water, high temperature and pressure, and acidity, as oil and gas wells become deeper and deeper. Some plugged wells have leaked and even caused serious environmental pollution and economic losses. For example, in two cruise studies in 2012 and 2013, three plugged wells in the North Sea of Norway all had bubbles continuously leaking into the ocean [2]. The industry, technology, and regulatory authorities have undergone some major changes in their attitudes towards permanent P&A in recent years due to the Macondo accident in 2010 and the subsequent serious oil spill [3].

Portland cement may not be ideal for permanent P&A operations that need to maintain long-term integrity. During the curing process, the material may shrink, crack, and mechanically and/or chemically degrade, resulting in oil and gas leakage into adjacent areas or the atmosphere [4]. This situation occurs because the cement may lose its hydrostatic balance before it is fully cured, allowing gas or liquid to migrate into the material, resulting in the formation of open channels and flow paths. In addition, cement may not be resistant to chemicals/substances. In old wells, cracks and micro-rings will form at the interface between the cement and the casing due to external forces generated during normal well operations, such as pressure testing and production.

* Corresponding author: sunruitao123@163.com

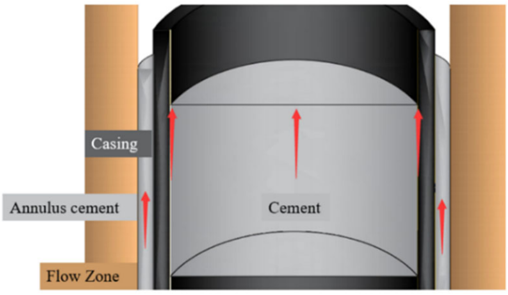

Figure. 1. Schematic diagram of cement sealing leakage path (left)

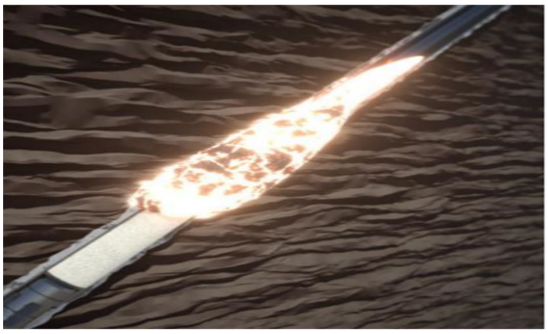

Figure. 2. Schematic diagram of the thermite P&A technology(right)

In order to solve the problems brought by the conventional well plugging and abandonment technology, a thermite plugging and abandonment technology is proposed in this field [5-7]. The thermite P&A technology is to use this heat to melt the components and rocks in the well, fuse the components in the well with the surrounding rocks, and form an impermeable barrier that runs through the entire cross section, as shown in Figure 1.
Now researchers have carried out numerical simulation research on this technology. Previous studies have focused on the temperature variation laws of the casing, cement, and rock formations[8-10]. At the same time, studies have shown that most of the energy released by thermite reaction is used to increase the internal power of casing and cement, which has little impact on rock formations. In order to study the direct influence of thermite reaction on the rock formation and its melting effect on the rock formation, experiments and numerical simulations were carried out.

2. Experiment

2.1 Experimental design

In order to study the direct influence of thermite reaction on the rock formation and its melting effect on the rock formation, experiments and numerical simulations were carried out.
The dosage of thermite is 2500g, and the compounding ratio of aluminum powder and iron oxide powder is 1:3. The nearly closed environment in Figure 1 is achieved by placing a plug in the central aperture. The diameter of the plug is 118mm, and the height is 30mm. The center of the plug has a hole with a diameter of 10mm, which is the activation channel of the aluminothermic reaction. The detailed data of this set of experiments are shown in Table 1.

Table 1 Experimental data

No.	Rock sample	Rock size(mm^3)	Center hole diameter (mm)	Center hole depth(mm)	Thermite weight(g)
1	sandstone	500×500×500	118	300	2500

3. Theory and Simulation

In order to study the effect of thermite reaction on the melting of rock formations, a two-dimensional axisymmetric heat conduction model was established. The structural schematic of the aluminothermic melting experiment is shown in Figure 3. R_{hole} is the radius of the cells containing the thermite mixture. $R_{sandstone}$ represents the thickness of the sandstone layer. The data for each layer of material is shown in Figure 1. The closed environment in which the thermite mixture is located refers to insulating material at one end and sandstone at the bottom of the hole at the other end.

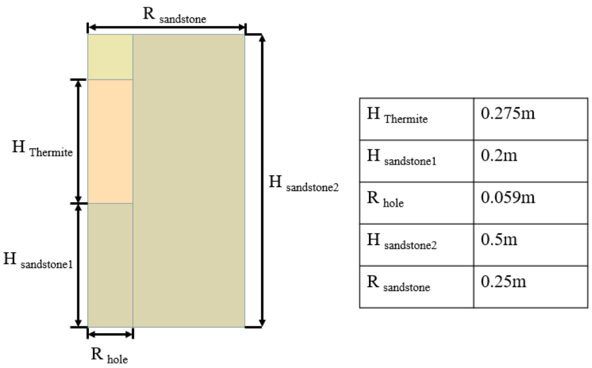

Figure. 3 Computational domain of aluminothermic melting structure (left)

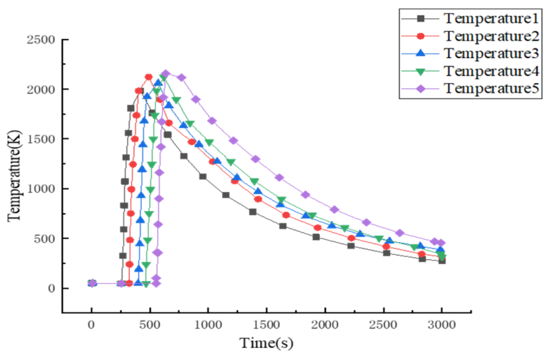

Figure. 4 Enhanced temperature curves (right)

Heat transfer studies utilizing the aluminothermic reaction to form plugs are still under development. There are few studies in the literature on the energy generated by the thermite reaction, especially considering the application to the formation of sealing plugs. At the same time, few studies on the direct influence of the thermite reaction on the temperature distribution and melting effect of the rock formation, so a model containing complex phenomena needs to be established. Therefore, to simplify the case, the following assumptions have been made:

a) Sandstone is considered to be homogeneous, without any porosity, and the physical parameters are constant.

b) Thermal contact resistance at the interface is ignored.

c) At the beginning of the calculation, we assumed that the temperature was uniform across the sandstone area.

d) The heat generated by the aluminothermic reaction approximates the heat flux distribution depending on space and time.

3.1 Heat conduction equation

Unsteady heat conduction is divided into periodic heat conduction and transient heat conduction. The transient thermal conduction process needs to be analyzed since only thermite melting effects are involved in this study. The following formula1 is the transient heat conduction equation, including phase transition.

$$\frac{\partial T}{\partial \mathrm{t}}=\frac{k}{\rho c}\left(\frac{\partial^2 T}{\partial x^2}+\frac{\partial^2 T}{\partial y^2}+\frac{\partial^2 T}{\partial z^2}\right)+\frac{Q_1}{\rho c} \tag{1}$$

where ρ is the density, kg/m^3; k is the thermal conductivity, W/(m·K) T is the temperature, °C; t represents a given time, s; Q_1 is the Heat source, W/m^3; c is Specific heat capacity, j/kg·°C.

Most heat conduction occurs in the thermite reaction range, so only heat conduction is considered in the thermite reaction range. The two-dimensional heat conduction equation is given based on the assumptions (formula 2).

$$\frac{\partial T}{\partial \mathrm{t}}=\frac{k}{\rho c}\left(\frac{\partial^2 T}{\partial r^2}+\frac{\partial^2 T}{\partial z^2}\right)+\frac{Q_1}{\rho c} \tag{2}$$

where r is the radius, m; $T = T = T(r,z,t)$; $\frac{\partial T}{\partial \mathrm{t}}\neq 0$;

No internal heat source, $Q_1=0$.

3.2 Convective Heat Transfer Model

Since the energy input used in the study was approximated by a transient heat flow curve estimated from the experimental data of Abdelal et al., the specific equation for the thermite reaction they considered is as formula 3.

$$8Al+3Fe_2O_3 \rightarrow 2Fe_3Al+3Al_2O_3 \tag{3}$$

In order to accurately solve the heat flux and heat flow through the sandstone, it is necessary to consider the convective heat loss involved in the entire heat transfer process. The following Newton cooling formulas (formula 4) are followed at different stages.

$$\begin{aligned} q_{\mathrm{con1}} &= h_1(T_{\mathrm{out}}-T_{air}), T_l > T_{air} \\ q_{\mathrm{con2}} &= h_2(T_l-T_s), T_l > T_s \\ q_{\mathrm{con3}} &= h_2(T_s-T_l), T_s > T_l \end{aligned} \tag{4}$$

where q is the heat transfer rate, W/m2; T_l is the fluid temperature, °C; T_s is the wall temperature, °C; T_{out} is the temperature of the outer surface of the thermocouple, °C; T_{air} is the air temperature, °C; h_1 is the heat transfer coefficient between fluid and air, W/m2·K; h_2 is the heat transfer coefficient between the fluid and the sandstone surface, W/m2·K.

3.3 Initial and Boundary Conditions

The initial conditions for applying the entire domain are as formula 5.

$$T(r,0)=T_{rock} \tag{5}$$

Where T_{rock} represents the temperature of the sandstone under standard conditions, and the temperature is uniformly distributed. Here, this temperature is 20°C, which is also used for the sandstone boundary condition. The boundary conditions are applied as formula 6.

$$\begin{aligned} &T(r,0,t)=T_{rock}, r_0<r<r_1 \\ &T(r,\mathrm{h},t)=T_{rock}, r_0<r<r_1 \\ &T(r_1,z,t)=T_{rock} \end{aligned} \tag{6}$$

Although the above equations define the boundary conditions, in order to be able to model the heat conduction effect of the thermite reaction, the heat flux input conditions need to be determined. Formula 7 has been given.

$$-k_{thermite}\frac{\partial T}{\partial r}=q_{input}(z,t) \tag{7}$$

At the insulating interface, formula 8 has been given.

$$-k_{thermite}\frac{\partial T}{\partial r}=0 \tag{8}$$

Since Abdelal et al. did not intend to melt the casing and other materials, the measured peak temperature of the thermite reaction was 912°C. In order to be able to study the melting effect of aluminothermic reaction on sandstone, an enhanced transient temperature profile method was adopted, as shown in Figure 4.

4. Results and discussion

4.1 Analysis of experimental results

The experimental procedure was recorded with a high-speed camera. The aluminothermic melting experiments under closed conditions are shown in Figure 5.

Figure. 5 The photo of the aluminothermic melting experiment

The melting experiment in a closed environment From Figure 9, the observed phenomenon of aluminothermic reaction can be observed. In order to keep the melting experiment process in a closed environment, this group of experiments adopts a sandstone plug as an approximation of a completely closed environment. As shown in Figure 5, the melting experiment under closed conditions is mainly divided into three stages. First, the thermite reaction in the sealing plug gradually increases the temperature of the thermite in the bottom hole. When the thermite reaction in the sealing plug is completed, the thermite at the bottom starts to react, as shown in Figure 5. From Figure 5, it can be seen that the reaction continues without a decreasing trend or the decreasing trend is relatively slow.

After cutting the molten experimental sample in a closed environment, peel off the product bonded to the inner wall of the hole, and observe the changes in the diameter and axial direction of the central hole of the sandstone. The results are shown in Figures 6 and 7.

Figure. 6 The diameter and height of the hole before and after the closed environment

As shown in Figures 6, the diameter of the sandstone hole in the closed environment is enlarged by about 10mm, and the axial direction is increased by about 17mm. By calculating the melting volume of sandstone, the melting volume of sandstone is about 1392cm^3.

4.2 Analysis of Numerical Simulation Results

The transient simulation analysis of the aluminothermic melting process is carried out through the solid and fluid heat transfer modules in the numerical simulation software. The numerical model parameters are set according to the parameters of the aluminothermic melting experiment, as shown in Figure 7.

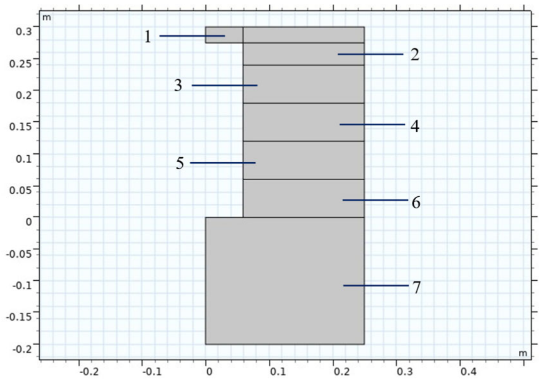

Figure. 7 Numerical model

In Figure 8, 1 represents the insulating material, which is used to simulate the closed environment of the experiment. The divided limestone represented by 2, 3, 4, 5, 6, and7 respectively corresponds to the temperature released by the aluminothermic reaction at different times. It is particularly noted that the five sets of data measured by Abdelal et al. by thermocouples did not specify the distance between the thermocouples, so the interval was assumed to be 5.5 cm in the numerical simulation.

Input the temperature boundary condition at the boundary to simulate the aluminothermic reaction process, and set the initial conditions of limestone and air. The thermite fusion model meshed with a total of 1303 elements. Measuring the peak temperature of each layer to observe the propagation of temperature and setting the simulation time was to 2000s. Due to the different combustion reaction times in different environments in the aluminothermic melting experiment, the time interval was set to 0-180 seconds and 180-3000 seconds. The time steps for each interval are 30 and 100 s, respectively. The corresponding temperature release law during the thermite reaction is shown in Figure 8.

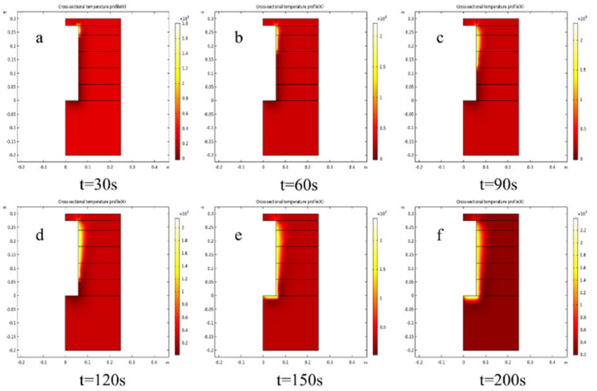

Figure. 8 Contour map of temperature transfer law: all stages of aluminothermic reaction

The temperature released by the thermite reaction is numerically simulated by entering the enhanced temperature boundary condition, as shown in Figure 9. Figure 9 show the variation of the temperature released by the aluminothermic reaction as a function of time and space. The reaction proceeds from top to bottom, and the release temperature also changes from top to bottom.
According to the temperature variation law shown in Figure 9, straight lines in different radial and axial directions are selected for numerical simulation of temperature. The selected straight lines are z=0.45m, z=0.425m, z=0.3375m, z=0.2325m, z=0.205m, y=0.064m, y=0.065m, r=0.03m.
The basis for selecting these straight lines is that they represent the temperature variation laws at different locations and are highly representative.

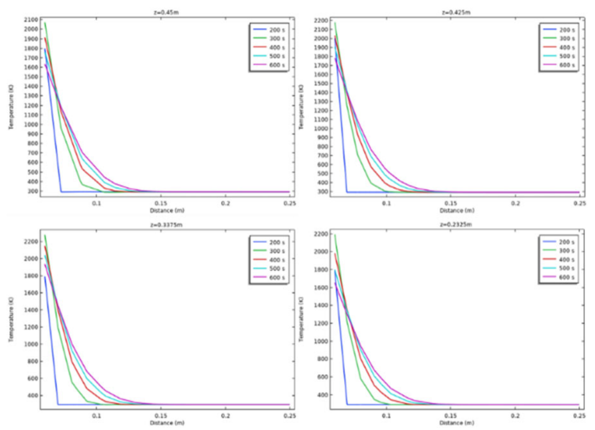

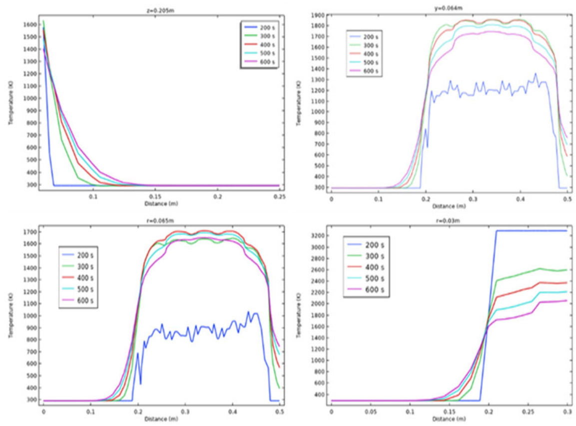

Figure. 9 Temperature variation in radial and axial directions: 200s~600s

It can be concluded from Figure 9 that at the beginning of the reaction, the temperature in different linear directions decreased sharply. The reason is that the temperature released by the aluminothermic reaction at this moment was only maintained for a moment, and the heat transfer in the sandstone was mainly concentrated on the inner wall of the hole. As time goes on, when t=300s, the temperature peaks are reached in each axial and radial direction. The maximum temperature of the inner wall of the hole is 2310K, which is the result of the continuous accumulation of energy released by the aluminothermic reaction. As time goes on, the peak temperatures in different straight-line directions gradually decrease with time. The reasons include the heat transfer between the molten product and the solid sandstone and the phase transition problems of the thermite and the sandstone.
It also can be concluded from Figure 9 that the temperature gradient will gradually decrease as the distance increases and gradually become stable. The temperature gradient also decreases first, increases with time, and finally becomes stable. At t=200s, at the boundary of r=0.064m temperature loading, the temperature increases and decreases sharply, and the maximum and minimum temperatures are 1390K and 293K, respectively. As the temperature of a part of the sandstone increases, the thermal resistance of the whole sandstone decreases. It may also be due to sandstone porosity and the existence of phase transition problems. The influence of insulating material and sandstone on the temperature transfer behavior of the aluminothermic reaction exists only at the boundary. With time, the peak temperature gradually decreased, but the changing trend remained unchanged. The melting range of sandstone is limited by the change of temperature with time and space, and the maximum melting range of sandstone is fixed at r=0.064m.

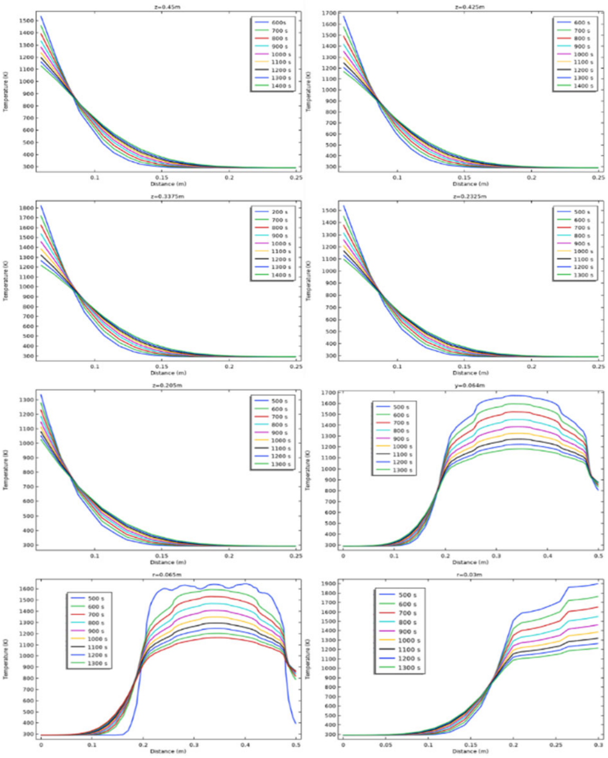

Figure. 10 Curve of temperature variation in radial and axial directions: 600s~1400s

It can be concluded from Figures 10 that the trend of temperature changes in the same straight line direction gradually weakens with the increase of time, and the curve of temperature changes with distance gradually becomes denser. This result is the temperature released by the aluminothermic reaction gradually tends to a stable value with time. The temperature values of the sandstone part and the molten material have reached a uniform distribution, resulting in a decrease in the temperature variation range.

As shown in Figure 10, when t=700s, the maximum value of the inner wall temperature of the hole in the direction of z=0.337m is 1830K, which still maintains high-efficiency heat transfer. Heat dissipation is more severe at both ends because the thermite is thermally insulating at one end and sandstone at one end. However, the effect on the z=0.337m direction is minimal, so the efficient heat transfer and melting effect are still maintained in this direction. For r=0.064m, r=0.065m, and r=0.03m, the maximum boundary temperature is 1680K, 1650K, and 1500K, respectively. These values are below the melting point of the sandstone, and the melting effect is insignificant, resulting in the melting product not maintaining heat transfer to the solid sandstone.

5. Conclusion

In this paper, the influence of the energy released by the aluminothermic reaction on the melting effect of sandstone is studied from the aspects of experimental design and theoretical analysis. The software simulates and calculates the temperature transfer law in different radial and axial directions.

The experimental results show that the energy released by the aluminothermic reaction has a noticeable effect on the melting of sandstone. After the experiment, the hole diameter of the sandstone was enlarged by 9.29mm, and the hole diameter was enlarged by 17.19mm in the axial direction.

A fluid-solid heat transfer model is established and analyzed based on the experimental design. Through analysis, we conclude that the heat transfer conditions around the aluminothermic reaction are the main factors affecting the temperature transfer in the sandstone. The maximum temperature at the top and bottom of the hole is significantly smaller than the temperature in the middle of the hole.

Therefore, we used software to simulate this model. From the simulation results, regardless of the time, the maximum temperature in the y=0.3375m direction is higher than the maximum temperature in other directions, and the maximum temperature can reach 2310K. The maximum melting ranges in the radial and axial directions are 0.064m and 0.189m, respectively.

The numerical simulation results are consistent with the experimental results, and the theoretical model has guiding significance for the practical exploration. Although the amount of the thermite will impact the peak temperature generated by the thermite reaction, its heat exchange environment plays a more important role here, affecting the melting effect of the thermite reaction on sandstone.

References

1. Achang M., Radonjic L.Y.A.M., "A Review of Past, Present, and Future Technologies for Permanent Plugging and Abandonment of Wellbores and Restoration of Subsurface Geologic Barriers," Environmental Engineering Science, vol. No.6(2020), pp. 395-408.
2. Vielstädte L.A., Karstens J.A., Haeckel M.A., Schmidt M.A., Linke P.A., Reimann S.A., Liebetrau V.A., McGinnis D.F.B.C., Wallmann K.A., "Quantification of methane emissions at abandoned gas wells in the Central North Sea(Article)," Marine and Petroleum Geology, vol. (2015), pp. 848-860.
3. Information on https://www.flopetrol-wb.com/plug-and-abandonment-pa-sandaband
4. Smith I., Shu D., "A STRATEGIC SHIFT IN WELL ABANDONMENT SERVICES," Oil and Gas Facilities, vol. No.1(2013).
5. Magalhães E.D.S.A., "A thermal study of a new oil well plugging & abandonment operation.," International Journal of Thermal Sciences, vol. (2020), pp. 106421.
6. d de Andrade G.S., de Lemos M.J.S., Colombo D., "A new hybrid analytical/numerical method for transient heat conduction in composite hollow cylinders applied to plug and abandonment of oil

wells," International journal of thermal sciences, vol. 168, no. (2021), pp. 106981.

7. Pena F.J.C., de Lemos CorresAuth CA CorresAuth Aemail Aemail M.J.S., "Unsteady heat conduction with phase change applied to a novel thermal plug and abandonment process," International Journal of Thermal Sciences, vol. (2021), pp. 107155.
8. Calvert D.G., "Issues and Techniques of Plugging and Abandonment of Oil and Gas Wells", in SPE Annual Technical Conference and Exhibition, New Orleans, Louisiana, 1994.
9. Kaiser M.K.M.J., Liu M.L.M., "Decommissioning cost estimation in the deepwater U.S. Gulf of Mexico - Fixed platformsand compliant towers(Article)," Marine Structures, vol. (2014), pp. 1-32.
10. Vrålstad T.T.V.S., "Plug & abandonment of offshore wells: Ensuring long-term well integrity and cost-efficiency (Review)," Journal of Petroleum Science and Engineering, vol. (2019), pp. 478-491.